Nickel Sulfate Induces Location-Dependent Atrophy of Mouse Olfactory Epithelium: Protective and Proliferative Role of Purinergic Receptor Activation

Cuihong Jia, Carlos Roman, and Colleen C. Hegg[1]

Department of Pharmacology and Toxicology, Michigan State University, East Lansing, Michigan 48824

[1] To whom correspondence should be addressed at Department of Pharmacology and Toxicology, B439 Life Sciences, Michigan State University, East Lansing, MI 48824. Fax: (517) 353-8915. E-mail: hegg@msu.edu.

Exposure to nickel sulfate ($NiSO_4$) leads to impaired olfaction and anosmia through an unknown mechanism. We tested the hypothesis that ATP is released following NiSO4-induced injury and that ATP promotes regenerative cell proliferation in the olfactory epithelium (OE). Male Swiss Webster mice were intranasally instilled with $NiSO_4$ or saline followed by ATP, purinergic receptor antagonists, or saline. We assessed the olfactory epithelium for $NiSO_4$-induced changes using histology and immunohistochemistry 1–7 days postinstillation and compared results to olfactory bulb ablation-induced toxicity. Intranasal instillation of $NiSO_4$ produced a dose- and time-dependent reduction in the thickness of turbinate OE. These reductions were due to sustentacular cell loss, measured by terminal dUTP nick-end labeling (TUNEL) staining at 1-day postinstillation and caspase-3–dependent apoptosis of olfactory sensory neurons at 3 days postinstillation. A significant increase in cell proliferation was observed at 5 and 7 days postinstillation of $NiSO_4$ evidenced by BrdU incorporation. Treatment with purinergic receptor antagonists significantly reduced $NiSO_4$-induced cell proliferation and posttreatment with ATP significantly increased cell proliferation. Furthermore, posttreatment with ATP had no effect on sustentacular cell viability but significantly reduced caspase-3–dependent neuronal apoptosis. In a bulbectomy-induced model of apoptosis, exogenous ATP produced a significant increase in cell proliferation that was not affected by purinergic receptor antagonists, suggesting that ATP is not released during bulbectomy-induced apoptosis. ATP is released following $NiSO_4$-induced apoptosis and has neuroproliferative and neuroprotective functions. These data provide therapeutic strategies to alleviate or cure the loss of olfactory function associated with exposure to nickel compounds.

Key Words: caspase-3; TUNEL; sustentacular cell; olfaction; purinergic receptor.

The mature mammal olfactory epithelium (OE) consists of three main cell compartments. The apical compartment contains a single layer of nonneuronal sustentacular cells which exhibit a great capacity for xenobiotic metabolism (Dahl and Hadley, 1991). The middle compartment contains several layers of olfactory sensory neurons (OSNs), the odorant-transducing cells that send axons to the olfactory bulb. The basal compartment adjacent to the basal lamina contains the basal progenitor cells that proliferate and give rise to sustentacular cells and OSNs continuously throughout adulthood under both physiological conditions or following injury (Graziadei and Monti-Graziadei, 1978). Cell proliferation in the OE is tightly regulated by multiple chemical signals produced by the different cells (Mackay-Sim and Chuah, 2000). Chemical, infectious, or traumatic damage to the OE disturbs the balance of these chemical signals and accelerates the rate of neurogenesis.

Occupational exposure to nickel sulfate ($NiSO_4$) occurs in ore refining, alloy and stainless steel production, nickel plating, and nickel-cadmium battery production (Tallkvist *et al*., 1998). Impaired olfaction and anosmia have been observed in humans exposed to soluble nickel compounds (Sunderman, 2001). Inhalation of soluble and insoluble nickel compounds leads to cellular lesions and atrophy in the OE of rodents (Benson *et al*., 1987). Evans et al. (1995) showed that inhalation of $NiSO_4$ significantly reduced the thickness of OE primarily due to the loss of the sustentacular cells but not the OSNs. Correspondingly, there are no changes in olfactory function measured by behavioral tasks (Evans *et al*., 1995), results that conflict with the human data showing anosmia. In this study, we investigated the mechanisms of soluble $NiSO_4$-induced toxicity and examined a potential mechanism of neuroprotection.

ATP, found in millimolar levels in all cells, promotes cell proliferation and neuroregeneration in the central nervous system (Neary and Zimmermann, 2009). ATP's activation of purinergic receptors upregulates antiapoptotic gene expression and downregulates proapoptotic gene expression, suggesting a neuroprotective role for ATP (Chorna *et al*., 2004). Activation of purinergic receptors by intranasal instillation of ATP induces cell proliferation and neuroregeneration in the

mouse OE (Jia *et al.*, 2009). Therefore, in the present study, we also investigated whether ATP is released following NiSO$_4$-induced injury to promote cell proliferation and to prevent cell death. The information from the present study will provide therapeutic strategies to alleviate, prevent, and cure the loss of olfactory function associated with occupational exposure to nickel compounds.

MATERIALS AND METHODS

Materials and animals. Materials were purchased from Sigma-Aldrich (St Louis, MO) unless otherwise specified. Adult male Swiss Webster mice (6–8 weeks) were purchased from Charles River (Portage, MI) and housed in a temperature-, humidity-, and light-controlled room (12 h light/dark cycle). Food and water were available *ad libitum*. All procedures were conducted in accordance with the Society of Toxicology's Guiding Principles in the Use of Animals in Toxicology and the National Institutes of Health Guide for the Care and Use of Laboratory Animals as approved by Michigan State University Institutional Animal Care and Use Committee.

In vivo studies. Anesthetized mice (4% isoflurane) were bilaterally instilled with saline vehicle or NiSO$_4$ (0.1, 0.5, or 2.5 mg/kg body weight) using a pipettor to place a total volume of 50 µl onto the nares. Mice were held in an upright position at least 1 min following instillation during the recovery from anesthesia, to insure that they inhaled the complete dose. We do not observe damage from repeated instillations. These *in vivo* doses, equivalent to 0.3, 1.5, and 7.6mM, approximate the cytotoxic concentration of 1mM previously used in *in vitro* studies (Li *et al.*, 2009; Zhou *et al.*, 2009). In some studies, purinergic receptor antagonists (suramin, 143 mg/kg, and pyridox-alphosphate-6-azophenyl-20, 40-disulfonic acid [PPADS], 30 mg/kg) or ATP (0.2 mg/kg) were instilled 30 min prior to NiSO$_4$ treatment and daily thereafter. In some studies, mice received three BrdU injections (ip, 180 mg/kg total) at 18, 20, and 22 h, and tissue was collected at 24 h after the last intranasal instillation as described below in the "Immunohistochemistry" section or in the "Western Blot" section ($n = 3$–4 mice per group).

To perform unilateral olfactory bulb ablation, mice were anesthetized (4% isoflurane to acquire anesthesia and then 2% isoflurane to maintain anesthesia), the scalp was incised, and a hole drilled through bone directly above the right olfactory bulb. The olfactory bulb was aspirated using a small diameter glass pipette, the hole packed with gelfoam, and the skin closed with surgical staples. The exposed bulb was left undamaged in sham animals. Tissue was collected and processed as described below in the "Immunohistochemistry" section.

Terminal dUTP nick-end labeling assay. Terminal dUTP nick-end labeling (TUNEL) was performed with In Situ Cell Death Detection Kit, TMR red (Roche, Indianapolis, IN) following manufacturer's instructions.

Immunohistochemistry. Vehicle- and NiSO$_4$-treated mice were anesthetized (65 mg/kg ketamine + 5 mg/kg xylazine, ip), transcardially perfused with ice-cold 0.1M PBS followed by 4% paraformaldehyde, and decapitated. The lower jaw and skin were removed and tissue was postfixed overnight in 4% paraformaldehyde. For the bulbectomy study, tissue was placed in RDO-Rapid Decalcifier for 4 h (Apex Engineering Products, Aurora, IL), and for the caspase-3 and TUNEL study, tissue was placed in 0.5M EDTA (pH 8.0) for 4–5 days. After decalcification, the tissues were cryoprotected with 20% sucrose and embedded in Tissue Tek OCT (Sakura Finetek, Torrance, CA). Frozen coronal sections of OE (20 µm) were collected from levels 2–6 of the mouse OE (Shipley *et al.*, 2003). Tissue was always compared from equivalent levels between treatment groups.

Tissue sections were rehydrated with 0.1M PBS, permeabilized with 0.3% Triton X-100, and blocked with 5% normal donkey serum (Jackson ImmunoResearch, West Grove, PA) in 0.1M phosphate-buffered saline for 1 h.

Tissue sections were incubated overnight at 4°C either singly or as a mixture with rabbit anticleaved caspase-3 antibody (ASP175; 1:200, Cell Signaling, Danvers, MA) and goat anti–olfactory marker protein (OMP) antibody (1:1000; Wako Chemical, Plano, TX) followed by incubation with fluorescein isothiocyanate-conjugated donkey anti-rabbit IgG and/or Cy3-conjugated donkey anti-goat IgG (1:200 and 1:50; Jackson ImmunoResearch Laboratory). BrdU immunohistochemistry was performed as described previously (Jia *et al.*, 2009). Nuclei were visualized by using mounting medium with 4′,6-diamidino-2-phenylindole (DAPI; Vector Laboratories, Burlingame, CA). Immunoreactivity was visualized on an Olympus FV1000 confocal microscope (Olympus, Center Valley, PA). No immunoreactivity was observed when the primary antibody or secondary antibody was omitted, providing evidence for antibody specificity. Standard hematoxylin and eosin (H&E) staining technique was used. The number of immunoreactive cells was manually counted by a single investigator blinded to the experimental conditions. Immunoreactive cells were counted from the septum, the endoturbinate II, and/or the ectoturbinate 2 from three tissue sections per animal (9–12 sections from three to four mice) as indicated in text. Quantification was at the tissue level where the endoturbinate 4 is first present (Fig. 1A). Data are expressed as number of immunoreactive cells per linear millimeter OE, measured using MetaMorph software (Molecular Devices, Downingtown, PA). Data were also evaluated as number of immunoreactive cells per millimeter square OE, to account for the decrease in thickness of the OE; however, there were no significant differences between the two analyses.

Western blot. Tissue was collected and homogenized as described previously (Jia *et al.*, 2009). Rabbit anti-cleaved caspase-3 (Asp175, 1:1000), rabbit anti-caspase-3 (1:1000; Cell Signaling), goat anti-OMP (1:2500; Wako Chemicals, Richmond, VA), or mouse anti-actin antibody (1:5000; Santa Cruz Biotechnology, Santa Cruz, CA) was used to probe for proteins, and immunoreactive proteins were detected as described previously (Jia *et al.*, 2009). Films were analyzed by Image J (http://rsbweb.nih.gov/ij/index.html; Wayne Rasband; NIH, Bethesda, MD). Integrated optimal density per microgram protein was expressed as a percentage of integrated optimal density per microgram protein of vehicle-treated animals. The value of activated caspase-3, caspase-3, and OMP for each animal was then normalized to the value of actin. Each sample was measured on three independent gels.

Statistical analysis. A one-way ANOVA followed by the Bonferroni post hoc test was performed using Prism 5 (GraphPad Software, San Diego, CA) unless specified otherwise. Significance was considered $p < 0.05$.

RESULTS

Morphological Effects of Intranasal Instillation of NiSO$_4$

We initially performed a dose-response study to investigate the effects of NiSO$_4$ (0.1, 0.5, and 2.5 mg/kg) on both turbinates and septum in adult mouse OE 4 days post-instillation. We performed histological H&E staining and measured the thickness of septum and turbinates (ectoturbinate 2 and endoturbinate II). We did not find significant alternations in the thickness of septum epithelium with any dose of NiSO$_4$ (Figs. 1B and 1C). However, compared to the vehicle control, 0.5 and 2.5 mg/kg NiSO$_4$ produced significant reductions in the thickness of turbinate epithelium (Figs. 1B and 1C; $p < 0.05$). To examine the time-dependent effect of NiSO$_4$ on the OE, we selected the 2.5-mg/kg NiSO$_4$ dose as it reduced the thickness of turbinates by 30–50%. Consistent with the dose-response study, there was no significant change observed in the septum at 1, 3, and 5 days postinstillation (Fig. 1D). However,
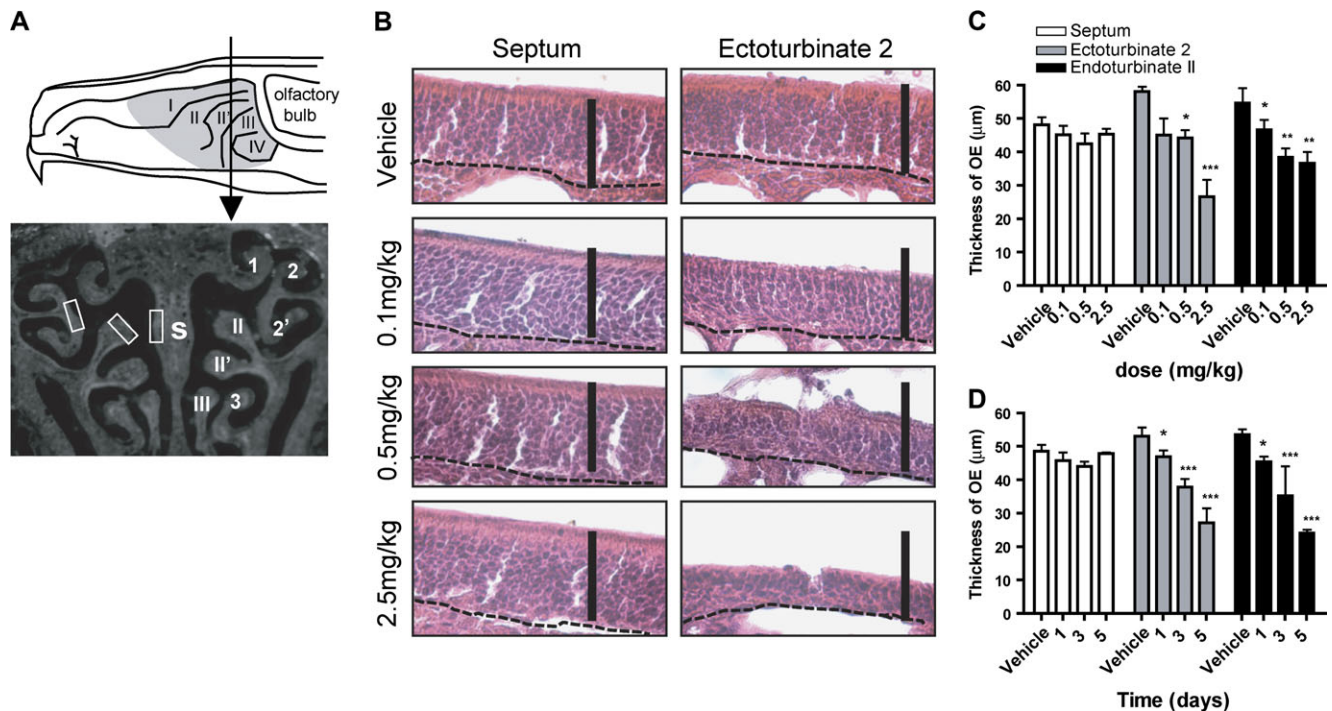
FIG. 1. NiSO₄ decreases the thickness of turbinate but not septal OE in adult mouse. (A) Top panel, schematic drawing of a sagittal plane through the rodent nasal cavity depicting the olfactory epithelium (gray shaded area) and level of tissue evaluated (arrow). Lower panel, image of the cross section taken at level indicated in top panel (arrow). Locations of endoturbinates (II, II', III), ectoturbinates (1, 2, 2', 3), and septum (s) are shown on right. White boxes indicate regions where thickness was measured (left). (B) H&E staining depicting the thickness of septum and ectoturbinate 2 at 4 days postinstillation of vehicle, 0.1, 0.25, and 2.5 mg/kg NiSO₄. Dashed lines delineate basal lamina. Scale bars = 50 μm. (C and D), Effect of dose (C) and time (D) on NiSO₄-induced changes in OE thickness. *$p < 0.05$, **$p < 0.01$, and ***$p < 0.001$.

compared to the vehicle control, the thickness of turbinates was significantly decreased at 1, 3, and 5 days postinstillation (Fig. 1D; $p < 0.05$). These data indicate that intranasal instillation of NiSO₄ produces dose- and time-dependent reductions in the thickness of turbinates but not septum in adult mouse OE.

NiSO₄ Induces Sustentacular Cell Death and OSN Apoptosis

To determine if the NiSO₄-induced decrease in the thickness of OE was due to apoptotic cell death, we performed the TUNEL assay to detect fragmentation of nuclear DNA that occurs during apoptosis in many cell types (Holcomb *et al.*, 1995). The number of TUNEL+ cells in vehicle-instilled animals was very low (Figs. 2A and 2D). Within 1 day of NiSO₄ instillation, there was a significant increase in TUNEL+ cells ($p < 0.001$). Most of the TUNEL+ cells were restricted to the apical sustentacular cell layer, but a few TUNEL+ cells were in the OSN and basal layers (Fig. 2B). At 3 days postinstillation, the number of TUNEL+ cells was still significantly increased compared to control (Figs. 2C and 2D; $p < 0.01$); however, the number of TUNEL+ cells was significantly reduced compared to 1 day (Fig. 2D, $p < 0.001$). At 3 days postinstillation, the TUNEL+ cells were located in the OSN and basal cell layer (Fig. 2C). These data indicate that

intranasal instillation of NiSO₄ induces maximal DNA fragmentation at 1 day that is predominately in the apical sustentacular cell layer.

We performed immunohistochemistry to measure the expression of activated caspase-3, used routinely to measure apoptotic-induced cell death. In the vehicle-treated group, we rarely observed activated caspase-3+ cells (Figs. 3B and 3M). Note that in the vehicle-treated group, the sustentacular cell layer consists of a row of highly packed large oval nuclei, labeled with DAPI (Fig. 3C), situated above the OSNs labeled with OMP (Fig. 3A). However, at 1-day postinstillation of NiSO₄ (Figs. 3D–F), the highly packed large oval nuclei of sustentacular cells were almost completely absent (Fig. 3F) from the apical layer above the OSN layer (Fig. 3D). These data are consistent with the observation of TUNEL+ cells in the sustentacular cell layer (Fig. 2B) and confirm that intranasal instillation of NiSO₄ produces sustentacular cell loss after 1 day. In addition, at 1 day and 3 days postinstillation, there was a significant increase in activated caspase-3+ cells (Fig. 3M; $p < 0.001$) that colocalized with OMP immunoreactivity in the OSN layer (Figs. 3D–I). In some cases, we also observed activated caspase-3+ immunoreactivity in the OMP+ nerve bundles in the lamina propria (Figs. 3G–I). At 5 days postinstillation (Figs. 3J–L), the number of activated
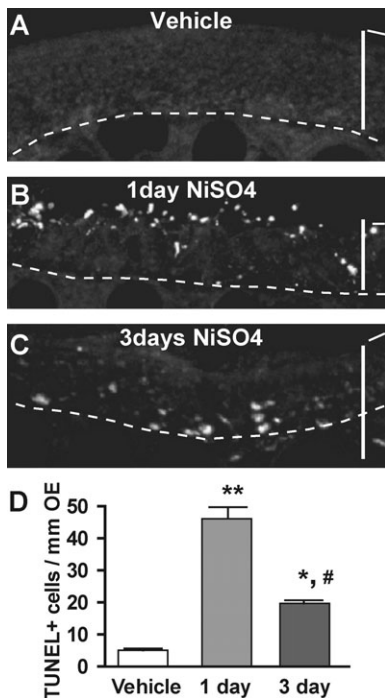
FIG. 2. NiSO$_4$-induced TUNEL staining in adult mouse OE. (A–C) TUNEL staining of DNA fragmentation following instillation of vehicle (0 mg/kg; A) or 2.5 mg/kg NiSO$_4$ at 1 day (B) or 3 days (C) postinstillation. Dashed lines delineate basal lamina. Scale bar = 50 µm. (D) Quantification of TUNEL+ cells in ectoturbinate 2 and endoturbinate II. *$p < 0.01$, **$p < 0.001$ versus vehicle control; #$p < 0.001$ versus 1 day.

caspase-3+ cells was significantly reduced to control levels (Fig. 3M; $p > 0.05$). OMP immunoreactivity in the middle OSN layer where the neuronal cell somas reside was also reduced and the appearance of the nerve bundles in the lamina propria, which contain the axons of the OSNs, was abnormal (Fig. 3J). We performed the Western blot technique to measure the protein levels of activated caspase-3 and OMP. Consistent with the immunohistochemical observations, the level of activated caspase-3 increased at 1 day and was significantly increased by 22-fold at 3 days postinstillation of NiSO$_4$ compared to the vehicle control (Figs. 4A and 4B; $p < 0.01$). Subsequently, the levels of caspase-3 and OMP were significantly decreased at 5 days postinstillation of NiSO$_4$ (Figs. 4C and 4D; caspase-3, $p < 0.01$; OMP, $p < 0.05$). To ascertain that the isoflurane anesthesia had no effect on caspase-3 activation (Xie et al., 2008) we examined control and isoflurane-exposed (4%, 1.5 min) frontal cortex, olfactory bulb, and olfactory epithelium 3 days postexposure. Western blot analysis did not reveal activated caspase-3 immunoreactivity in either the control or isoflurane-exposed tissue, suggesting that in the time period that we examined, isoflurane did not appreciably activate caspase-3 (data not shown). Collectively, we conclude that intranasal instillation of NiSO$_4$ produces sustentacular cell loss at 1 day followed by caspase-3–dependent OSN apoptosis at 3 days in adult mouse OE.

Increased Cell Proliferation following NiSO$_4$-Induced Injury

We examined cell proliferation in the turbinates at 3, 5, and 7 days postinstillation of 2.5 mg/kg NiSO$_4$ in animals pretreated with saline via the BrdU incorporation assay. BrdU incorporation was not significantly changed 3 days postinstillation of NiSO$_4$ compared to 0-day vehicle control ($p > 0.05$) but was significantly increased at 5 and 7 days postinstillation (Figs. 5A–E; $p < 0.001$). There was no significant difference in the number of BrdU+ cells at 5 and 7 days postinstillation ($p > 0.05$). These data indicate that progenitor cell proliferation occurs between 3 and 5 days postinstillation of NiSO$_4$.

ATP Mediates Increased Cell Proliferation in NiSO$_4$-Induced Injury

Our previous studies showed that ATP, via activation of purinergic receptors, induces cell proliferation in normal mouse OE (Jia et al., 2009). Therefore, we hypothesized that ATP is released and promotes cell proliferation following NiSO$_4$-induced injury in the OE. In order to test this hypothesis, we intranasally instilled purinergic receptor antagonists (PPADS + suramin) 30 min before NiSO$_4$ instillation and daily thereafter. There was a significant increase in BrdU+ cells at 7 days postinstillation in P2 antagonist-treated groups compared to 0-day vehicle control (Figs. 5E–H; $p < 0.01$). However, BrdU+ cells in the purinergic antagonist-treated group were significantly reduced at 5 and 7 days postinstillation compared to the saline-pretreated NiSO$_4$ groups (Figs. 5B–D) ($p < 0.05$). These data indicate that inhibition of purinergic receptors significantly reduces NiSO$_4$-induced increases in cell proliferation in the OE, suggesting that ATP could be released to promote cell proliferation via activation of purinergic receptors. In addition, we intranasally instilled ATP daily after NiSO$_4$. BrdU+ cells in ATP-treated animals were significantly increased at 5 and 7 days postinstillation (Figs. 5E, J–L; $p < 0.01$ vs. saline). These data indicate that intranasal instillation of exogenous ATP potentiates NiSO$_4$-induced cell proliferation in the OE. Consistent with time-dependent morphological changes following NiSO$_4$ in the saline-treated animals (Fig. 1D), we observed time-dependent decreases of turbinate OE thickness in saline-, purinergic antagonist-, and ATP-treated animals (Fig. 5I; $p < 0.001$ compared to 0-day vehicle control). Collectively, these data strongly suggest that ATP is released and promotes cell proliferation following NiSO$_4$-induced injury in the adult mouse OE.

ATP Is Antiapoptotic to OSNs but not Sustentacular Cells

ATP has a neuroprotective role and reduces apoptosis in the central nervous system (CNS) (Chorna et al., 2004). Therefore, we investigated whether ATP has a neuroprotective role in NiSO$_4$-induced injury. Daily instillation of ATP following NiSO$_4$ instillation had no significant effect on the number of TUNEL+ cells at both 1 day and 3 days compared to the saline-treated group (Fig. 6A; $p > 0.05$).
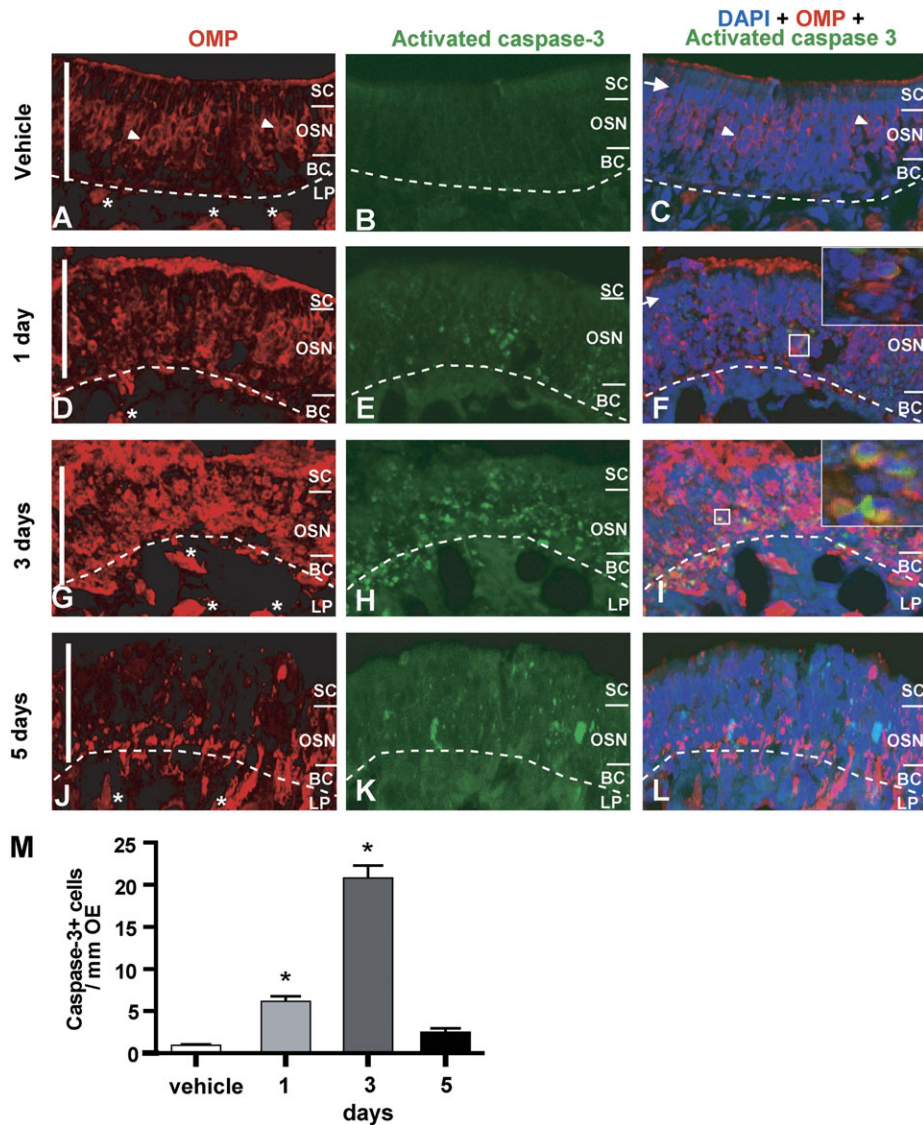
FIG. 3. NiSO₄ induces caspase-3–dependent OSN apoptosis. (A–L) Triple labeling of OSNs with OMP (A, D, G, J), activated caspase-3 (B, E, H, K), and nuclei with DAPI (C, F, I, L), in animals treated with vehicle (A–C, endoturbinate II), or after 1 (D–F, ectoturbinate 2), 3 (G–I, ectoturbinate 2), or 5 days (J–L, ectoturbinate 2) NiSO₄ (2.5 mg/kg) instillation. Dashed lines delineate basal lamina. Scale bar = 50 μm. SC, sustentacular cell layer, OSN, OSN layer, BC, basal cell layer, LP, lamina propria. Arrow indicates tightly packed large oval nuclei of sustentacular cells. Arrow heads indicate small round nuclei of OMP+ OSNs. ''*'' Indicates OMP-positive nerve bundle in LP. Inset—(F and I) expanded regions (white squares) depict colocalization of activated caspase-3 and OMP in the OSN layer. (M) Quantification of caspase-3+ cells in turbinates. *$p < 0.001$.

This result agrees with our previous observations that NiSO₄ induces an increase in TUNEL+ cells predominantly in the sustentacular cell layer at 1 day but also to a lesser extent in the OSN layer at 3 days (Fig. 2D). Thus, intranasal instillation of ATP does not prevent or reduce NiSO₄-induced sustentacular cell loss mediated via DNA fragmentation. Compared to the saline-treated group, daily instillation of ATP following NiSO₄ instillation had no significant effect on the number of activated caspase-3+ cells at 1 day (Fig. 6B; $p > 0.05$) but produced a significant reduction at 3 days (Fig. 6B; $p < 0.05$). These data are consistent with our previous observation that NiSO₄ induces activated caspase-3 expression that peaks at 3 days postinstillation of NiSO₄ (Fig. 3M). As the loss of OSNs occurs at 3 days post-NiSO₄ treatment, these data suggest that intranasal instillation of ATP prevents or reduces NiSO₄-induced caspase-3–dependent apoptosis of OSNs. Taken together, these data indicate that ATP prevents or reduces NiSO₄-induced OSN apoptosis but not sustentacular cell loss mediated by DNA fragmentation in adult mouse OE.
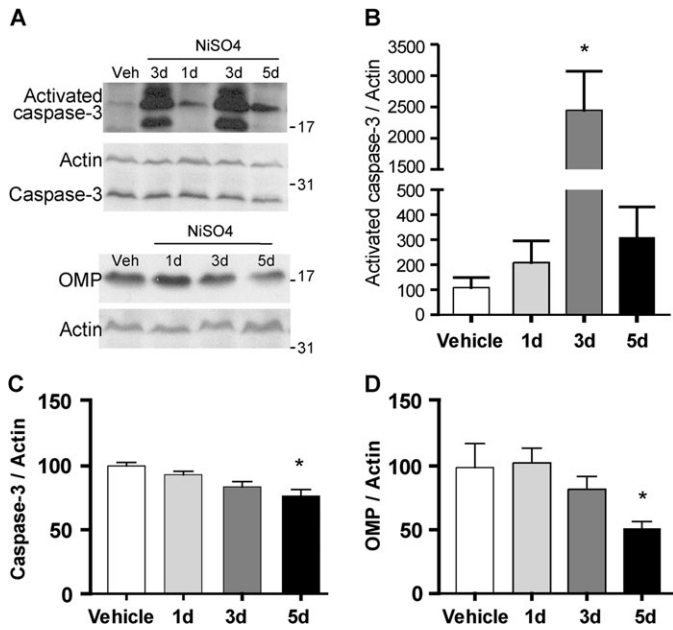
FIG. 4. Effect of $NiSO_4$ on activated caspase-3 protein levels. (A) Representative immunoblot of activated caspase-3, caspase-3, OMP, and actin in vehicle- and $NiSO_4$ (2.5 mg/kg)-instilled animals. (B–D) Quantification of activated caspase-3, caspase-3, and OMP. *$p < 0.05$.

ATP Potentiates Cell Proliferation following Bulbectomy-Induced Apoptosis

In order to determine if release of ATP following apoptosis is a universal mechanism of toxicity that promotes regeneration, we examined other models of OSN apoptosis. Olfactory bulb ablation induces caspase-3–dependent OSN apoptosis (Cowan and Roskams, 2002); thus, we performed unilateral bulbectomies in adult mice and measured the levels of BrdU incorporation. BrdU+ cells in the saline-treated animals were significantly increased at 2, 4, 6, and 8 days after surgery compared to sham treatment (Fig. 7A; $p < 0.001$). Intranasal instillation of purinergic receptor antagonists did not alter the levels of BrdU+ cells at any day monitored compared to saline-treated groups (Fig. 7A). These data suggest that either ATP is not released or purinergic receptors are not involved in bulbectomy-induced cell proliferation. In order to examine whether purinergic receptors mediate bulbectomy-induced cell proliferation, we intranasally instilled ATP following bulbectomy and found that ATP significantly increased the BrdU+ cells in the OE at 6 and 8 days (Fig. 7A; $p < 0.001$), indicating that activation of purinergic receptors potentiates bulbectomy-induced cell proliferation in the OE. Collectively, these data indicate that ATP is not released during bulbectomy-induced OSN apoptosis. Although bulbectomy does not directly induce sustentacular cell death, evidence suggests that morphological changes in sustentacular cells may contribute to the regeneration following bulbectomy (Makino et al., 2009). Therefore, we monitored proliferation of sustentacular cells after bulbectomy. Compared to sham animals, the levels of BrdU+ cells in the sustentacular cell layer were significantly increased 4–8 days after surgery ($p < 0.05$) in all groups (Figs. 7A and 7B). In ATP-treated groups, BrdU incorporation was significantly greater than saline-treated groups at 8 days after surgery ($p < 0.001$). These data suggest that ATP potentiates sustentacular cell regeneration following bulbectomy in adult mouse OE.
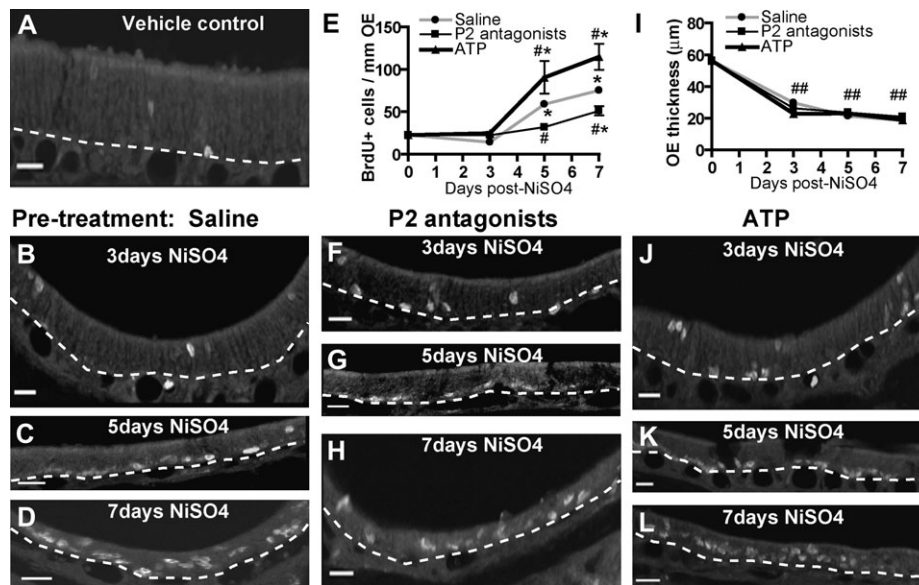

FIG. 5. Effect of ATP and purinergic receptor antagonists on $NiSO_4$-induced cell proliferation. BrdU immunoreactivity in the turbinates of animals treated with (A) 0 mg/kg $NiSO_4$ (0 day), (B–D) saline vehicle, (F–H) purinergic receptor antagonists, or (J–L) ATP following instillation of $NiSO_4$ (2.5 mg/kg) at 3, 5, or 7 days postinstillation. Dashed lines delineate basal lamina. Scale bar = 10 μm. (E and I) Quantification of BrdU+ cells (E) or OE thickness (I) in turbinates. *$p < 0.01$ versus vehicle control (two-way ANOVA). #$p < 0.05$ and ##$p < 0.01$ versus saline/$NiSO_4$-treated animals (two-way ANOVA).
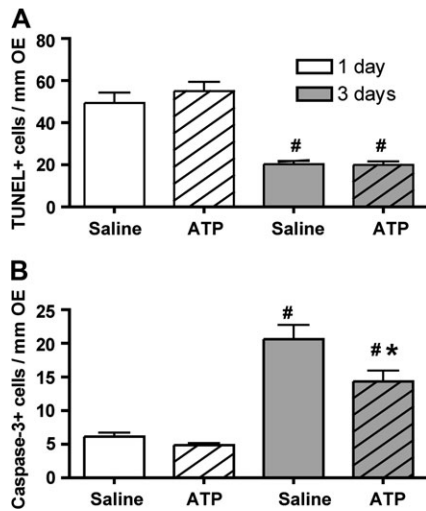
FIG. 6. Effect of ATP on NiSO$_4$-induced apoptosis. Quantification of (A) TUNEL+ cells and (B) activated caspase-3+ cells in ectoturbinate 2 and endoturbinate II. $^{#}p < 0.05$ versus respective 1-day group. $*p < 0.05$ versus 3 days saline control.

In contrast to cell proliferation, the thickness of the OE was significantly decreased in all treatment groups after bulbectomy ($p < 0.001$) compared to sham animals. There were no significant differences among saline, purinergic receptor antagonists, and ATP treatment. In addition, we observed significant decreases in the thickness of OE in the unlesioned side 2–8 days after bulbectomy (Fig. 7C). There were no differences of these effects among vehicle, purinergic receptor antagonists, or ATP treatments, indicating that this effect is due to nonspecific effects of surgery.

DISCUSSION

The results from the present study show that intranasal instillation of NiSO$_4$ produces location-dependent atrophy of OE measured by the dose- and time-dependent reductions in the thickness of turbinate but not septal OE in adult mouse. These reductions were due to sustentacular cell loss, as measured by TUNEL staining at 1 day postinstillation, and caspase-3–dependent apoptosis of OSNs at 3 days post-instillation. Following cell death, BrdU-incorporated cell proliferation was significantly increased at 5 and 7 days post-NiSO$_4$ instillation. Treatment with purinergic receptor antagonists significantly reduced NiSO$_4$-induced cell proliferation, while posttreatment with ATP significantly potentiated NiSO$_4$-induced cell proliferation. These data indicate that ATP is released and promotes cell proliferation in NiSO$_4$-induced injury. We were unable to distinguish the cell type that releases ATP following NiSO$_4$ exposure. All cells contain millimolar levels of ATP which could be released following injury. We speculate that the sustentacular cells, the first cells damaged, release ATP initially; however, we cannot exclude
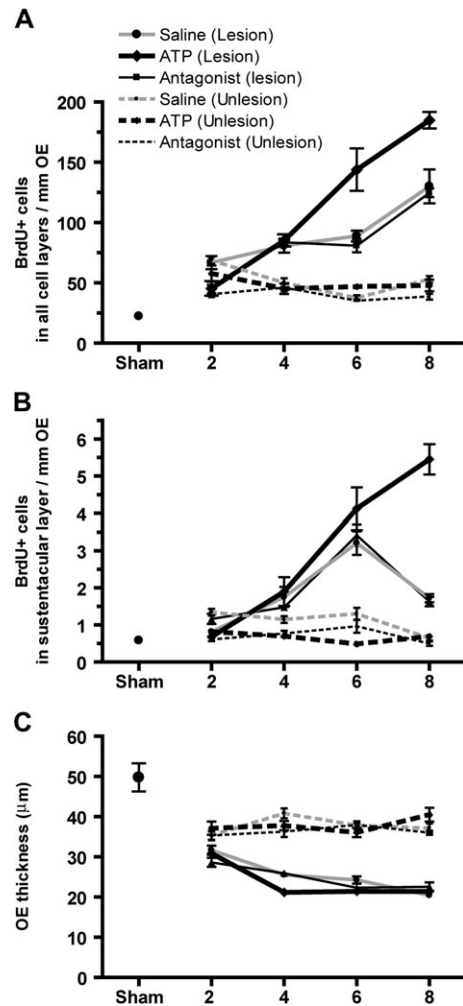

FIG. 7. Effect of ATP on bulbectomy-induced apoptosis. Quantification of BrdU+ cells in all cell layers of the turbinates (A) or in the apical sustentacular cell layer (B). (C) Quantification of bulbectomy-induced decreases in the thickness of OE in the turbinates. Solid lines indicate lesioned side and dashed lines indicate unlesioned side. $*p < 0.05$ versus sham and $^{#}p < 0.001$ versus vehicle (two-way ANOVA followed by Bonferroni post hoc test).

the possibility that other cells types also release ATP. Further experiments are warranted to ascertain the source of ATP.

The neuroproliferative effects of ATP following injury were further supported by a bulbectomy model in which we found that exogenous ATP potentiated bulbectomy-induced cell proliferation. However, in this model, purinergic receptor antagonists had no effect on cell proliferation, suggesting that ATP is not endogenously released following bulbectomy. Finally, posttreatment with ATP following NiSO$_4$ had no effect on sustentacular cell viability but significantly reduced caspase-3–dependent neuronal apoptosis, indicating that ATP prevents or reduces NiSO$_4$-induced OSN apoptosis in the OE. Taken together, these data indicate that ATP is released and has neuroproliferative and neuroprotective functions in NiSO$_4$-induced OE injury.

$NiSO_4$-Induced Cell Death: Sustentacular Cell versus OSN

Our study of the effects of intranasal instillation of $NiSO_4$ in mouse OE is in agreement with the study by Evans *et al.* (1995) in which inhalation of $NiSO_4$ significantly reduced sustentacular cells in rat OE. This observed toxicity in the sustentacular cells could result either from local damage and/or a selective susceptibility of sustentacular cells to $NiSO_4$. Sustentacular cell somas are situated in the apical portion of the epithelium and form a protective barrier for the rest of the OE. In addition, there is a zone of tight junctions close to the apical surface (Menco, 1980) that prevents paracellular diffusion of lipophobic compounds. In this way, the sustentacular cells may be damaged due to high local concentrations of $NiSO_4$ that do not have access to other cell types in the OE. In support of this hypothesis, we see greater atrophy with increasing doses of $NiSO_4$. In addition, Ni^{2+} induces the formation of the hydroxyl radical (Torreilles and Guerin, 1990) which can evoke single DNA strand breaks and DNA-protein cross-links (Patierno and Costa, 1985), consistent with our observation of DNA fragmentation in sustentacular cells 1 day postinstillation of $NiSO_4$. However, Evans *et al.* (1995) hypothesized that the mechanism of $NiSO_4$-induced sustentacular cell loss could be attributed to the expression of metabolic enzymes as biotransformation enzymes are preferentially expressed in sustentacular cells (Banger *et al.*, 1994). $NiSO_4$ can inhibit many metabolic enzymes (Maines and Kappas, 1977) including superoxide dismutase, which results in increased formation of intracellular free radicals resulting in oxidative stress (Shainkin-Kestenbaum *et al.*, 1991).

As previously reported in rat (Evans *et al.*, 1995), Ni^{2+} did not significantly reduce numbers of OSNs in the mouse septal area; however, we found a significant decrease in OSNs at 3 and 5 days postinstillation of $NiSO_4$ in the turbinates, a region not examined by Evans *et al.* (1995). We hypothesize that the $NiSO_4$-induced damage to the olfactory neurons is secondary to the damage in the sustentacular cells, based on the reduction in OSNs 2–4 days following the loss of sustentacular cells. Sustentacular cells function to isolate the OSNs, providing structural support and possible trophic support. Thus, the loss of the sustentacular cells could cause a delayed loss of OSNs, as was observed in this study.

The hyposmia and anosmia observed in occupational nickel exposure could be explained by nickel-induced effects to neurons. $NiSO_4$ reportedly induces apoptosis via activation of death receptor 3 and caspase-8, leading to activation of caspase-3 (Zhao *et al.*, 2009). $NiSO_4$-induced OSN apoptosis in the present study could be through a similar death receptor/caspase-8–mediated mechanism. In addition, Ni^{2+} reduces odorant-induced calcium transients in the dendritic knob, the dendrite, and the soma of OSNs via inhibition of T-type Ca^{2+} channels (Gautam *et al.*, 2007). Calcium has an important role in odorant signal transduction. Odorant activation of G-protein receptors located on the cilia increases cyclic AMP and causes calcium influx via cyclic nucleotide–gated channels with subsequent activation of calcium-dependent chloride channels. The depolarization caused by calcium influx and chloride efflux travels to the cell soma where action potentials are produced. T-type channels are thought to contribute to the spread of depolarization from the knob to the cell soma (Gautam *et al.*, 2007). Thus, nickel, by inhibition of the T-type channels, may inhibit odorant signal transduction that ultimately leads to hyposmia and anosmia.

$NiSO_4$-Induced Atrophy: Turbinates versus Septum

In this study, we observed atrophy of the OE following instillation of aqueous $NiSO_4$, supporting earlier studies in which the thickness of septal OE was significantly reduced following inhalation of $NiSO_4$ (635 $\mu g/m^3$) (Evans *et al.*, 1995). Evans *et al.* (1995) monitored the septal OE directly targeted by normal airflow patterns in the rat (Morgan and Monticello, 1990). However, turbulent airflow enhances gas absorption around the turbinates (Morgan and Monticello, 1990), and thus, inhalation of $NiSO_4$ could produce atrophy in the turbinate OE (Evans *et al.*, 1995; Sunderman, 2001). In the present study, we examined $NiSO_4$-induced atrophy in the entire OE including ectoturbinate 2, endoturbinate II, and septum. We found that intranasal instillation of $NiSO_4$ produced a dose- and time-dependent reduction in the thickness of turbinate but not septal OE. The disparity between our results and previous observations could be due to differences in regional deposition of $NiSO_4$ with exposure routes or local tissue susceptibility. Both mechanisms have been reported to influence nasal lesion distribution (Morgan and Monticello, 1990). In a preliminary experiment, we intranasally instilled 50 μl trypan blue (4% solution) to document the distribution of intranasal instillation. We found that the majority of trypan blue staining was located on the turbinates and that there was sparse staining located along the septum and dorsal medial meatus (Supplementary fig. 1). Therefore, the absence of atrophy in septal OE in $NiSO_4$-instilled animals could be due to a lack of deposition of $NiSO_4$.

Alternatively, local tissue susceptibility could affect the distribution of $NiSO_4$-induced atrophy. Previous studies show an increased occurrence of lesions in the turbinates compared to septal OE following exposure to toxicants (Cassee and Feron, 1994; Genter *et al.*, 1995). In the OE, there are high concentrations of both phase I cytochrome P450 and phase II biotransformation enzymes (Banger *et al.*, 1994; Chen *et al.*, 1992) that are distributed in specific zones in the OE (Whitby-Logan *et al.*, 2004). Many biotransformation enzymes are inhibited by nickel (Maines and Kappas, 1977), and as mentioned above, nickel can inhibit superoxide dismutase, a superoxide scavenging enzyme, thereby increasing the production of reactive oxygen species (Shainkin-Kestenbaum *et al.*, 1991). Indeed, region-specific damage of OE correlates with the localization of biotransformation enzymes (Brittebo, 1993).

Therefore, NiSO$_4$-induced OE atrophy in turbinates observed in the present study could be attributed to the differential expression of biotransformation enzymes in turbinates.

Neuroproliferative and Neuroprotective Roles of ATP

In the CNS, ATP is released upon injury and exerts multiple trophic actions via activation of purinergic receptors, including proliferation, neuronal differentiation, survival, and apoptosis (Neary and Zimmermann, 2009). Recent data indicate that ATP is also involved in homeostatic regulation in the OE. Activation of purinergic receptors evokes the release of trophic factors (Kanekar *et al.*, 2009) and increases in OSN proliferation in mouse (Jia *et al.*, 2009) and tadpole (Hassenklöver, 2009). ATP also upregulates heat shock protein expression (Hegg and Lucero, 2006), suggesting that ATP initiates a stress signaling cascade to facilitate cell survival. Here, we found that ATP potentiates cell proliferation following NiSO$_4$- and bulbectomy-induced damage and decreases NiSO$_4$-induced OSN apoptosis. Taken together, these data demonstrate that ATP has neuro-proliferative and neuroprotective roles in normal and injured OE.

Interestingly, the toxic effects of nickel observed in the present study, in which an acute, single instillation of nickel was administered to mice, are similar to a study in which rats were exposed chronically, 6 h/day for 16 days via inhalation (Evans *et al.*, 1995). This suggests that ATP may also have a neuroproliferative and neuroprotective effect on OE chronically exposed to nickel. Some toxicants, particularly methyl bromide (Hurtt *et al.*, 1988), also annihilate the sustentacular cells and neurons in the OE but spare the basal progenitor cells. Our previous results indicate that purinergic receptors are expressed by the basal cells (Hegg *et al.*, 2003) and that ATP increases basal cell proliferation (Jia *et al.*, 2009). Thus, the sustentacular cells and neurons could release ATP immediately following toxicant exposure prior to cell death and depletion, thereby inducing the basal cells to proliferate. Other toxicants, including ZnSO$_4$ (Schultz, 1960) and Triton X-100 (Verhaagen *et al.*, 1990), kill all cell types. In this situation, in the absence of the proliferative basal cells, we do not predict that the epithelium would be responsive to ATP. Overall, this study provides the purinergic system as a therapeutic target to alleviate or restore the loss of olfactory function associated with occupational exposure to nickel compounds.

SUPPLEMENTARY DATA

Supplementary data are available online at http://toxsci .oxfordjournals.org/.

FUNDING

ACKNOWLEDGMENTS

REFERENCES

Banger, K. K., Foster, J. R., Lock, E. A., and Reed, C. J. (1994). Immunohistochemical localisation of six glutathione S-transferases within the nasal cavity of the rat. *Arch. Toxicol.* **69,** 91–98.

Benson, J. M., Carpenter, R. L., Hahn, F. F., Haley, P. J., Hanson, R. L., Hobbs, C. H., Pickrell, J. A., and Dunnick, J. K. (1987). Comparative inhalation toxicity of nickel subsulfide to F344/N rats and B6C3F1 mice exposed for 12 days. *Fundam. Appl. Toxicol.* **9,** 251–265.

Brittebo, E. B. (1993). Metabolism of xenobiotics in the nasal olfactory mucosa: implications for local toxicity. *Pharmacol. Toxicol.* **72**(Suppl. 3), 50–52.

Cassee, F. R., and Feron, V. J. (1994). Biochemical and histopathological changes in nasal epithelium of rats after 3-day intermittent exposure to form-aldehyde and ozone alone or in combination. *Toxicol. Lett.* **72,** 257–268.

Chen, Y., Getchell, M. L., Ding, X., and Getchell, T. V. (1992). Immunolocalization of two cytochrome P450 isozymes in rat nasal chemosensory tissue. *Neuroreport* **3,** 749–752.

Chorna, N. E., Santiago-Perez, L. I., Erb, L., Seye, C. I., Neary, J. T., Sun, G. Y., Weisman, G. A., and Gonzalez, F. A. (2004). P2Y receptors activate neuroprotective mechanisms in astrocytic cells. *J. Neurochem.* **91,** 119–132.

Cowan, C. M., and Roskams, A. J. (2002). Apoptosis in the mature and developing olfactory neuroepithelium. *Microsc. Res. Tech.* **58,** 204–215.

Dahl, A. R., and Hadley, W. M. (1991). Nasal cavity enzymes involved in xenobiotic metabolism: effects on the toxicity of inhalants. *Crit. Rev. Toxicol.* **21,** 345–372.

Evans, J. E., Miller, M. L., Andringa, A., and Hastings, L. (1995). Behavioral, histological, and neurochemical effects of nickel (II) on the rat olfactory system. *Toxicol. Appl. Pharmacol.* **130,** 209–220.

Gautam, S. H., Otsuguro, K. I., Ito, S., Saito, T., and Habara, Y. (2007). T-type Ca2+ channels mediate propagation of odor-induced Ca2+ transients in rat olfactory receptor neurons. *Neuroscience* **144,** 702–713.

Genter, M. B., Owens, D. M., and Deamer, N. J. (1995). Distribution of microsomal epoxide hydrolase and glutathione S-transferase in the rat olfactory mucosa: relevance to distribution of lesions caused by systemically-administered olfactory toxicants. *Chem. Senses* **20,** 385–392.

Graziadei, P. P. C., and Monti-Graziadei, G. A. (1978). *Continuous Nerve Cell Renewal in the Olfactory System* (M. Jacobson, Ed.), pp. 55–83. Springer, New York.

Hassenklöver, T. (2009). Purinergic signaling regulates cell proliferation of olfactory epithelium progenitors. *Stem Cells* **27,** 2022–2031.

Hegg, C. C., Greenwood, D., Huang, W., Han, P., and Lucero, M. T. (2003). Activation of purinergic receptor subtypes modulates odor sensitivity. *J. Neurosci.* **23,** 8291–8301.

Hegg, C. C., and Lucero, M. T. (2006). Purinergic receptor antagonists inhibit odorant-induced heat shock protein 25 induction in mouse olfactory epithelium. *Glia* **53,** 182–190.

Holcomb, J. D., Mumm, J. S., and Calof, A. L. (1995). Apoptosis in the neuronal lineage of the mouse olfactory epithelium: regulation *in vivo* and in vitro. *Dev. Biol.* **172,** 307–323.

Hurtt, M. E., Thomas, D. A., Working, P. K., Monticello, T. M., and Morgan, K. T. (1988). Degeneration and regeneration of the olfactory epithelium following inhalation exposure to methyl bromide: pathology, cell kinetics, and olfactory function. *Toxicol. Appl. Pharmacol.* **94,** 311–328.

Jia, C., Doherty, J. D., Crudgington, S., and Hegg, C. C. (2009). Activation of purinergic receptors induces proliferation and neuronal differentiation in Swiss Webster mouse olfactory epithelium. *Neuroscience* **163,** 120–128.

Kanekar, S., Jia, C., and Hegg, C. C. (2009). Purinergic receptor activation evokes neurotrophic factor neuropeptide Y release from neonatal mouse olfactory epithelial slices. *J. Neurosci. Res.* **87,** 1424–1434.

Li, Q., Suen, T. C., Sun, H., Arita, A., and Costa, M. (2009). Nickel compounds induce apoptosis in human bronchial epithelial Beas-2B cells by activation of c-Myc through ERK pathway. *Toxicol. Appl. Pharmacol.* **235,** 191–198.

Mackay-Sim, A., and Chuah, M. I. (2000). Neurotrophic factors in the primary olfactory pathway. *Prog. Neurobiol.* **62,** 527–559.

Maines, M. D., and Kappas, A. (1977). Regulation of cytochrome P-450-dependent microsomal drug-metabolizing enzymes by nickel, cobalt, and iron. *Clin. Pharmacol. Ther.* **22,** 780–790.

Makino, N., Ookawara, S., Katoh, K., Ohta, Y., Ichikawa, M., and Ichimura, K. (2009). The morphological change of supporting cells in the olfactory epithelium after bulbectomy. *Chem. Senses* **34,** 171–179.

Menco, B. P. (1980). Qualitative and quantitative freeze-fracture studies on olfactory and nasal respiratory epithelial surfaces of frog, ox, rat, and dog. III. Tight-junctions. *Cell Tissue Res.* **211,** 361–373.

Morgan, K. T., and Monticello, T. M. (1990). Airflow, gas deposition, and lesion distribution in the nasal passages. *Environ. Health Perspect.* **85,** 209–218.

Neary, J. T., and Zimmermann, H. (2009). Trophic functions of nucleotides in the central nervous system. *Trends Neurosci.* **32,** 189–198.

Patierno, S. R., and Costa, M. (1985). DNA-protein cross-links induced by nickel compounds in intact cultured mammalian cells. *Chem. Biol. Interact.* **55,** 75–91.

Schultz, E. W. (1960). Repair of the olfactory mucosa with special reference to regeneration of olfactory cells (sensory neurons). *Am. J. Pathol.* **37,** 1–19.

Shainkin-Kestenbaum, R., Caruso, C., and Berlyne, G. M. (1991). Effect of nickel on oxygen free radical metabolism. Inhibition of superoxide dismutase and enhancement of hydroxydopamine autoxidation. *Biol. Trace Elem. Res.* **28,** 213–221.

Shipley, M. T., Puche, A. C., and Ennis, M. (2003). *The Olfactory System* (G. Paxinos, Ed). Academic press NY.

Sunderman, F. W., Jr. (2001). Nasal toxicity, carcinogenicity, and olfactory uptake of metals. *Ann. Clin. Lab. Sci.* **31,** 3–24.

Tallkvist, J., Henriksson, J., d'Argy, R., and Tjalve, H. (1998). Transport and subcellular distribution of nickel in the olfactory system of pikes and rats. *Toxicol. Sci.* **43,** 196–203.

Torreilles, J., and Guerin, M. C. (1990). Nickel (II) as a temporary catalyst for hydroxyl radical generation. *FEBS Lett.* **272,** 58–60.

Verhaagen, J., Oestreicher, A. B., Grillo, M., Khew-Goodall, Y. S., Gispen, W. H., and Margolis, F. L. (1990). Neuroplasticity in the olfactory system: Differential effects of central and peripheral lesions of the primary olfactory pathway on the expression of B-50/GAP43 and the olfactory marker protein. *J. Neurosci. Res.* **26,** 31–44.

Whitby-Logan, G. K., Weech, M., and Walters, E. (2004). Zonal expression and activity of glutathione S-transferase enzymes in the mouse olfactory mucosa. *Brain Res.* **995,** 151–157.

Xie, Z., Culley, D. J., Dong, Y., Zhang, G., Zhang, B., Moir, R. D., Frosch, M. P., Crosby, G., and Tanzi, R. E. (2008). The common inhalation anesthetic isoflurane induces caspase activation and increases amyloid beta-protein level *in vivo. Ann. Neurol.* **64,** 618–627.

Zhao, J., Bowman, L., Zhang, X., Shi, X., Jiang, B., Castranova, V., and Ding, M. (2009). Metallic nickel nano- and fine particles induce JB6 cell apoptosis through a caspase-8/AIF mediated cytochrome c-independent pathway. *J. Nanobiotechnol.* **7,** 2.

Zhou, X., Li, Q., Arita, A., Sun, H., and Costa, M. (2009). Effects of nickel, chromate, and arsenite on histone 3 lysine methylation. *Toxicol. Appl. Pharmacol.* **236,** 78–84.